THE JOURNAL OF BIOLOGICAL CHEMISTRY VOL. 291, NO. 31, pp. 16208–16220, July 29, 2016

Role of Conserved Disulfide Bridges and Aromatic Residues in Extracellular Loop 2 of Chemokine Receptor CCR8 for Chemokine and Small Molecule Binding*

Received for publication, November 26, 2015, and in revised form, May 18, 2016 Published, JBC Papers in Press, May 19, 2016, DOI 10.1074/jbc.M115.706747

Line Barington[‡], Pia C. Rummel[‡], Michael Lückmann[‡§], Heidi Pihl[‡], Olav Larsen[‡], Viktorija Daugvilaite[‡], Anders H. Johnsen[¶], Thomas M. Frimurer[§‖], Stefanie Karlshøj[‡], and Mette M. Rosenkilde[‡1]

From the [‡]Department of Neuroscience and Pharmacology, the [§]Novo Nordisk Foundation Center for Basic Metabolic Research, and the [‖]Novo Nordisk Foundation Center for Protein Research, University of Copenhagen, DK-2200 Copenhagen, Denmark and the [¶]Department of Clinical Biochemistry, Rigshospitalet, DK-2100 Copenhagen, Denmark

Chemokine receptors play important roles in the immune system and are linked to several human diseases. The initial contact of chemokines with their receptors depends on highly specified extracellular receptor features. Here we investigate the importance of conserved extracellular disulfide bridges and aromatic residues in extracellular loop 2 (ECL-2) for ligand binding and activation in the chemokine receptor CCR8. We used inositol 1,4,5-trisphosphate accumulation and radioligand binding experiments to determine the impact of receptor mutagenesis on both chemokine and small molecule agonist and antagonist binding and action in CCR8. We find that the seven-transmembrane (TM) receptor conserved disulfide bridge (7TM bridge) linking transmembrane helix III (TMIII) and ECL-2 is crucial for chemokine and small molecule action, whereas the chemokine receptor conserved disulfide bridge between the N terminus and TMVII is needed only for chemokines. Furthermore, we find that two distinct aromatic residues in ECL-2, Tyr^{184} (Cys + 1) and Tyr^{187} (Cys + 4), are crucial for binding of the CC chemokines CCL1 (agonist) and MC148 (antagonist), respectively, but not for small molecule binding. Finally, using *in silico* modeling, we predict an aromatic cluster of interaction partners for Tyr^{187} in TMIV (Phe^{171}) and TMV (Trp^{194}). We show *in vitro* that these residues are crucial for the binding and action of MC148, thus supporting their participation in an aromatic cluster with Tyr^{187}. This aromatic cluster appears to be present in a large number of CC chemokine receptors and thereby could play a more general role to be exploited in future drug development targeting these receptors.

Chemokines (chemotactic cytokines) regulate the differentiation, activation, and recruitment of leukocytes. They also play important roles in several physiological mechanisms outside the immune system such as organogenesis and angiogenesis (1, 2). With ~50 members, these cytokines exert their effects through chemokine receptors (23 members), which belong to class A of the family of seven-transmembrane (7TM)[2] G protein-coupled receptors (3). The implications of the chemokine system in a vast number of human diseases (3) have increased the interest in developing potent, selective, and clinically useful chemokine receptor antagonists.

The binding of a chemokine to its cognate receptor is initially driven by electrostatic interactions between the overall positively charged chemokine and the negatively charged extracellular surface of the receptor. Then interactions between the chemokine N terminus and residues in the main binding pocket of the receptor trigger receptor activation (4–6). In contrast, small molecule ligands bind deeper in the main binding pocket and constrain the receptors in either active or inactive conformations (7, 8). Whereas most mapping studies of small molecules have focused on the transmembrane areas, newer studies as well as crystal structures of class A receptors suggest that extracellular receptor regions, in particular extracellular loop (ECL)-2, participate directly or indirectly in ligand binding (9–14).

In class A receptors, ECL-2 is the largest and most divergent of the extracellular loops, and crystal structures show how it adopts very different conformations between receptor subclasses (10–14). A disulfide bridge between cysteine residues in the extracellular end of transmembrane helix (TM) III and the middle of ECL-2 is present in almost all 7TM receptors and is thus termed the 7TM receptor conserved disulfide bridge (denoted 7TM bridge). In addition, nearly all endogenous chemokine receptors (except CXCR6) have another disulfide bridge, the chemokine receptor conserved disulfide bridge (CKR bridge), between cysteine residues in the N terminus and in what was earlier believed to be ECL-3. However, from novel crystal structures, it is evident that this second cysteine is located in the top of TMVII (13, 15–17). Most recently, crystal structures of P2Y1R and P2Y12R (Protein Data Bank codes 4XNW and 4PXZ) have been solved, indicating that the presence of this disulfide bridge is not limited to the chemokine receptor family (18, 19).

* This work was supported by Det Frie Forskningsråd, Hørslev-Fonden, Lundbeckfonden, Novo Nordisk, Novo Nordisk Foundation Center for Basic Metabolic Research, and NovoNordisk Foundation Center for Protein Research. The authors declare that they have no conflicts of interest with the contents of this article.

[1] To whom correspondence should be addressed: Dept. of Neuroscience and Pharmacology, University of Copenhagen, Panum Institute Bldg. 18.5, Blegdamsvej 3B, DK-2200 Copenhagen, Denmark. Tel.: 45-30604608; E-mail: rosenkilde@sund.ku.dk.

[2] The abbreviations used are: 7TM, seven-transmembrane; 7TM bridge, 7TM receptor conserved disulfide bridge; Bip, bipyridine; CKR bridge, chemokine receptor conserved disulfide bridge; ECL, extracellular loop; IP_3, inositol 1,4,5-trisphosphate; Phe, phenanthroline; TM, transmembrane helix; LMD-A, *N*-(5-[*N*-((3*R*,4*R*)-1-((S)-2-aminopropanoyl)-3-methyl-piperidine-4-yl)sulfamoyl)naphthalene-1-yl]-2-methylbenzamide; ICM, internal coordinate mechanics.

CCR8 is selectively expressed on regulatory T cells and a subset of T helper 2 cells and is up-regulated on the latter upon activation (20). Accordingly, several studies have suggested a role for CCR8 in diseases like asthma, atopic dermatitis, and anaphylaxis (20–22). Until recently, only one endogenous ligand, CCL1, was known to activate CCR8. However, in 2013, CCL18 was proposed as another, less potent CCR8 ligand (23). Additional virus-encoded CC-chemokines targeting CCR8 have been described, including the CCR8-specific antagonist MC148, encoded by the poxvirus *Molluscum contagiosum* (24, 25).

The association of CCR8 with the diseases mentioned above has sparked the interest in CCR8 as a potential drug target. In recent years, several CCR8 antagonists have been described, including oxazolidinone-based (26), naphthalene-sulfonamide-based (27, 28), and diazaspiroundecane-based (29) antagonists. Furthermore, CCR8 is targeted by various small molecule agonists (9, 30, 31).

Here we describe the importance of certain extracellular areas of CCR8 for the interaction with and action of both peptide and non-peptide agonists and antagonists. In addition to the two disulfide bridges, the importance of selected aromatic amino acids located C-terminal to the conserved cysteine in ECL-2 was also tested. Our studies suggest that ECL-2 is important for proper chemokine-CCR8 interactions. A homology model of CCR8 indicated the presence of an aromatic cluster of residues involving Tyr^{187} on position Cys + 4 (4 positions C-terminal to the conserved cysteine, Cys^{183}) in ECL-2 and residues in the top of TMIV and TMV. These *in silico* data were confirmed *in vitro*.

Results

The Conserved Disulfide Bridges Are Important for Chemokine-mediated Activation of CCR8—To test the importance of the two disulfide bridges, the 7TM receptor conserved disulfide bridge (7TM bridge) and the chemokine receptor conserved disulfide bridge (CKR bridge) (Fig. 1*A*), for ligand binding to and activation of CCR8, each bridge was disrupted by substituting cysteine with alanine residues. Four mutants were generated: C106A and C183A, which have a disrupted 7TM bridge, and C25A and C272A, lacking the CKR bridge. Cell surface expression of the mutant receptors was tested by ELISA. Mutant receptors lacking the CKR bridge (C25A and C272A) were expressed at levels comparable with (or slightly higher than) the WT receptor, whereas mutants lacking the 7TM bridge (C106A and C183A) had up to 6-fold decreased surface expression (Fig. 1*B*). Confocal microscopy of fluorescently stained receptors supported the expression levels determined by ELISA (Fig. 1, *C–E*). The importance of the two bridges for chemokine-induced activation of CCR8 was then investigated using an IP_3 accumulation assay. In this assay, the $G\alpha_i$ signal from CCR8 was converted into a $G\alpha_q$ response by co-transfecting the cells with the chimeric G protein $G\alpha_{\Delta 6qi4myr}$ (32). This allows measurements of the $G\alpha_i$ signaling of CCR8 ($G\alpha_i$ inhibits adenylate cyclase, and the $G\alpha_i$ activity is measured as inhibition of forskolin-induced cAMP production) into a $G\alpha_q$ signal ($G\alpha_q$ activates phospholipase C, and the activity is measured as IP_3 accumulation) without interference with the receptor structure but only by interference with the G protein downstream of the receptor.

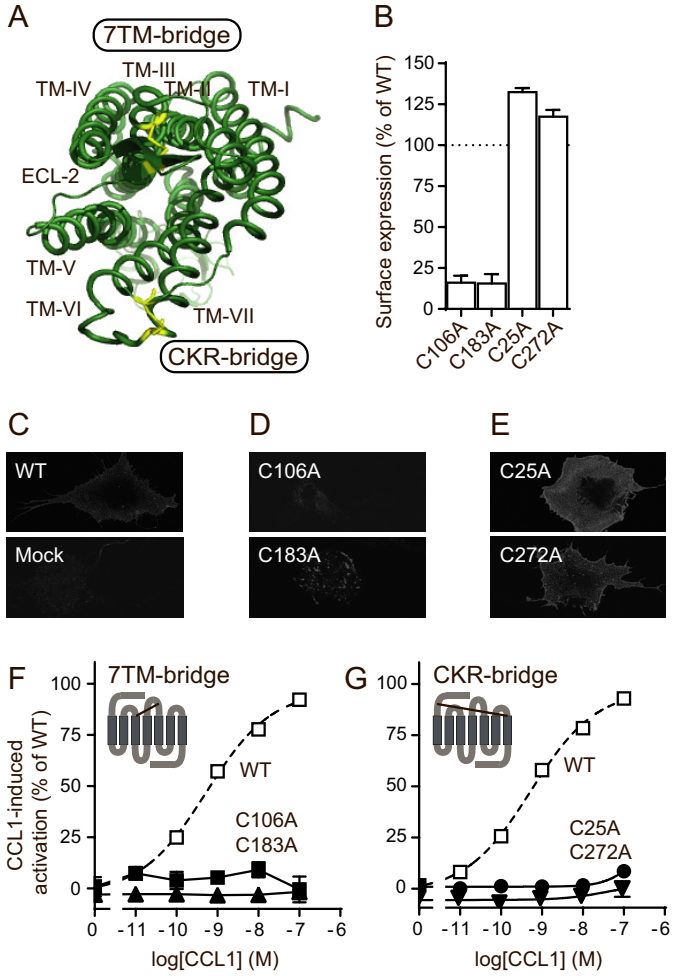

FIGURE 1. **Importance of conserved disulfide bridges for CCR8 cell surface expression and CCL1-induced activation.** *A*, crystal structure of CCR5 (top view, Protein Data Bank code 4MBS), highlighting the two disulfide bridges in *yellow*. The figure was made using PyMOL software. *B*, surface expression of the four mutant receptors, as tested by ELISA ($n = 3–4$). The data were normalized to the expression level of CCR8 WT (100%, mean $A_{450} = 0.415 \pm 0.039$) and empty vector (0%, mean $A_{450} = 0.135 \pm 0.02$). *C–E*, representative confocal microscopy images of COS-7 cells transiently transfected with the indicated constructs. *C*, CCR8 WT and pcDNA empty vector (mock). *D*, C106A and C183A. *E*, C25A and C272A. *F* and *G*, IP_3 accumulation experiments in transiently transfected COS-7 cells that show activation with CCL1 of CCR8 mutants lacking the 7TM receptor conserved disulfide bridge (*F*) or the chemokine receptor conserved disulfide bridge (*G*). A schematic representation of the relevant bridge is shown as an *inset* in each panel. The data were normalized to CCR8 WT activation (*dotted line*). The average maximal WT count (100%) was 5093 ± 885 cpm, and the average empty vector count (0%) was 639 ± 136 cpm. The *error bars* (barely visible) represent S.E. ($n = 4–5$ for the mutants and $n = 33$ for the WT).

The CCR8-specific chemokine CCL1 was not able to activate any of the mutants (Fig. 1, *F* and *G*). To validate the approach with co-transfection of CCR8 with the chimeric $G\alpha_{\Delta 6qi4myr}$, we compared the CCL1-induced signaling of CCR8 WT measured by this approach with the CCL1-induced inhibition of forskolin-induced cAMP formation measured by cAMP levels. Similar potencies were obtained in these two pathways (data not shown).

Chemokine Binding to CCR8 Is Dependent on Both Disulfide Bridges—To investigate the mechanism responsible for the lack of activation, the binding of CCL1 to the CCR8 mutants was

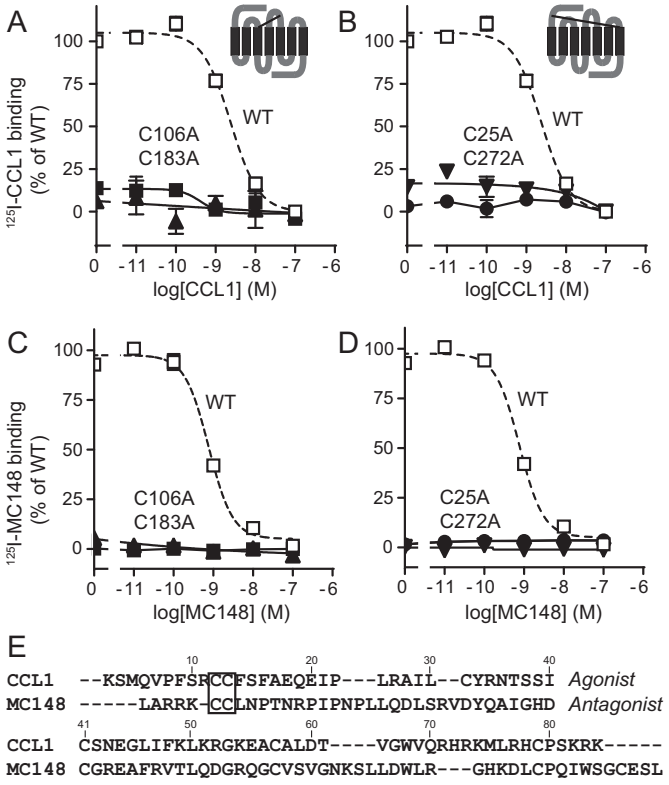

FIGURE 2. **Importance of conserved disulfide bridges for chemokine binding to CCR8.** *A–D*, homologous competition binding experiments in transiently transfected COS-7 cells. Binding of ^{125}I-CCL1 (*A* and *B*) or ^{125}I-MC148 (*C* and *D*) to CCR8 mutants with disrupted 7TM receptor conserved bridge (*A* and *C*) or chemokine receptor conserved bridge (*B* and *D*) is shown. The data were normalized to WT binding, which is represented by a *dotted line*. In CCL1 experiments, the average maximal count for the WT (100%) was 1965 ± 105 cpm, and the average count for the empty vector (0%) was 788 ± 46 cpm. In MC148 experiments, the average maximal count for the WT was 605 ± 62 cpm, and the average count for the empty vector was 63 ± 10 cpm. *Error bars* represent S.E. ($n = 3–5$). Schematic representations of the relevant bridge are shown as *insets* in *A* and *B*. *E*, alignment using CLUSTALW 1.7 of the sequences of the agonist CCL1 and the antagonist MC148 (25). The CC motif in both chemokines is highlighted with a *box*.

tested in homologous competition binding experiments. ^{125}I-CCL1 did not bind to any of the mutant receptors (Fig. 2, *A* and *B*), explaining the lack of receptor activation. We next took advantage of a CCR8-specific CC-chemokine antagonist, the human poxvirus-encoded MC148, to test whether a CC-chemokine antagonist is also dependent upon the disulfide bridges. Like ^{125}I-CCL1, no binding was observed for ^{125}I-MC148 (Fig. 2, *C* and *D*), indicating that both bridges are central for CC-chemokine agonist, as well as antagonist binding to CCR8. A comparison between the amino acid sequences of CCL1 and MC148 is given in Fig. 2*E*.

Small Molecule Action in CCR8 Is Dependent upon the 7TM but Not the CKR bridge—As just seen, the lack of activation of the mutant receptors by CCL1 could be explained by a lack of chemokine binding. However, from those data it remains unknown whether the chemokine binding event alone is inhibited or whether the potential for receptor activation *per se* is also inhibited. To investigate this, small molecule agonists were tested for their abilities to activate the mutant receptors. We used the metal ion chelator complexes bipyridine (Bip) and phenanthroline (Phe) in complex with zinc and copper (ZnBip, CuBip, ZnPhe, and CuPhe), which have been shown to activate CCR8 with micromolar potencies (31, 33). These agonists bind to deeply located residues in the main binding pocket and are expected to be independent on extracellular receptor regions (34, 35). The 7TM bridge was found to be important for small molecule-mediated activation, because alanine substitution of either Cys^{106} or Cys^{183} totally abolished activation, as exemplified by CuPhe (Fig. 3*A*). In contrast, receptors lacking the CKR bridge were activated by the small molecule agonists, including CuPhe (Fig. 3*B*), with WT-like potencies, and CuPhe-induced activation was inhibited in these mutants by the highly potent naphthalene sulfonamide-based small molecule antagonist LMD-A (28) like in the WT receptor (Fig. 3*C*).

Tyr^{184} (Cys + 1) in ECL-2b Is Required for CCL1-mediated but Not Small Molecule-mediated Activation of CCR8—As demonstrated above, the 7TM bridge is essential for chemokine and small molecule action and thus seems to be important for receptor activation *per se*. One of the cysteine residues participating in the 7TM bridge (Cys^{183} in CCR8) divides ECL-2 into two parts: ECL-2a, which is the N-terminal part, and the C-terminal part ECL-2b (Fig. 4). Even though ECL-2 is the most divergent loop in class A 7TM receptors, aromatic amino acids are conserved in ECL-2b at position Cys + 4 in the family of CC-chemokine receptors, where 9 of 10 receptors have an aromatic residue (Fig. 4). In CCR8, aromatic residues are found at positions Cys + 1, Cys + 3, and Cys + 4. We previously reported that these aromatic amino acids (Tyr^{184}, Phe^{186}, and Tyr^{187}, respectively) are differentially important for the activation of CCR8 by CCL1 (9). Here, we compare those previous findings for the CC-chemokine agonist CCL1 with new data for the CC-chemokine antagonist MC148 and small molecule agonists (metal-ion chelator complexes) and antagonist (LMD-A).

As reported previously (9), the potency of CCL1-induced activation of CCR8 Y184A was highly impaired (Fig. 5*A* and Table 1), and there was a smaller, but significant, decrease in potency for F186A (Fig. 5*B* and Table 1). In contrast, CCL1 activated Y187A with WT-like potency, albeit with a marked decrease in efficacy (Fig. 5*C* and Table 1). Four small molecule agonists, as exemplified by CuPhe (Fig. 5, *D–F*), activated all three CCR8 mutants with WT-like potencies. The surface expression of the mutants was ~70% of that of the WT for Y184A, ~100% of the WT for F186A, and ~50% for Y187A (Table 1).

Tyr^{187} (Cys + 4) in ECL-2b Is Central for CC-chemokine-mediated but Not Small Molecule-mediated CCR8 Inhibition—The two chemically different antagonists, *i.e.* the CC-chemokine antagonist MC148 and the small molecule antagonist LMD-A, were next tested for their abilities to inhibit CCL1-induced activation in the absence of the aromatic residues. Surprisingly, Tyr^{187} (Cys + 4) was found to be essential for the action of MC148, whereas this chemokine acted independently of Phe^{186} and was only slightly affected by the lack of Tyr^{184} (Fig. 6, *A–C*). In contrast, LMD-A was only affected by the loss of Tyr^{187}, but this residue was not essential for its action (Fig. 6, *D–F*).

The Binding of CC-chemokine Agonist and Antagonist to CCR8 Depends upon Two Distinct Aromatic Residues in ECL-2b—The functional studies uncovered that Tyr^{184} was central for chemokine-mediated activation of CCR8 (Fig. 5*A*) but not for CCR8 activation *per se* (because the small molecule

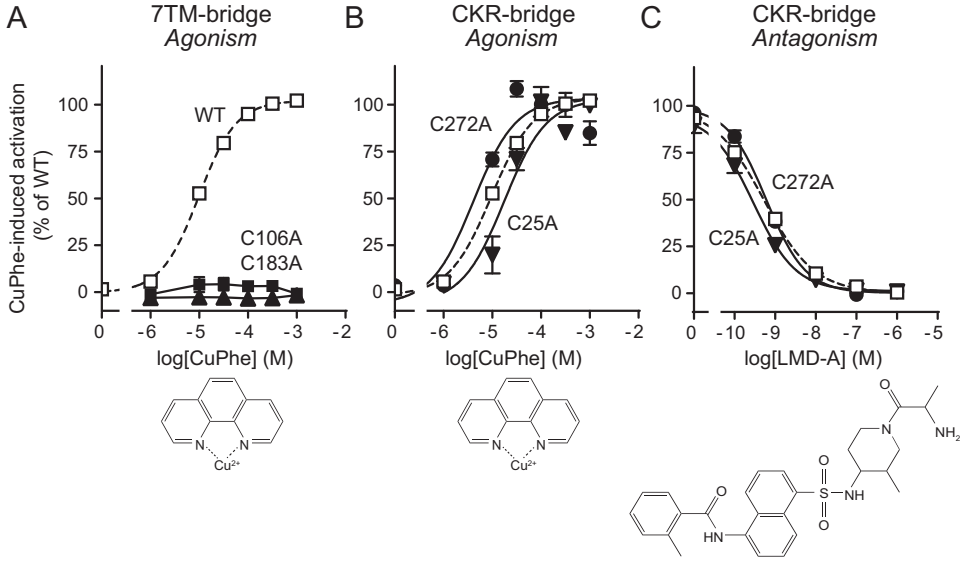

FIGURE 3. **Importance of disulfide bridges for small molecule agonist and antagonist actions in CCR8.** IP_3 accumulation experiments in transiently transfected COS-7 cells. *A* and *B*, CuPhe-induced activation of mutant receptors lacking the 7TM receptor conserved disulfide bridge (*A*) or the chemokine receptor conserved disulfide bridge (*B*). *C*, effect of the small molecule antagonist LMD-A on CuPhe-induced activation of mutant receptors lacking the chemokine receptor conserved disulfide bridge. The data were normalized to WT activation. The average maximal count for the CuPhe-induced activation of the WT (100%) was 4042 ± 42 cpm, and the average count for the empty vector (0%) was 882 ± 49 cpm. The *error bars* represent S.E. (n = 3–5 for the mutants and n = 20 for the WT). The molecular structure of the relevant ligand, either CuPhe (39) or LMD-A (28), is shown below each panel.

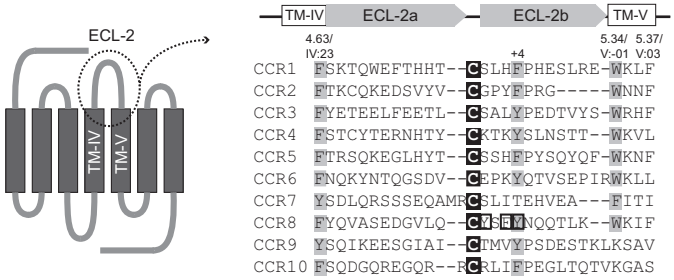

FIGURE 4. **Aromatic amino acids in the ECL-2 region of human CC-chemokine receptors.** Alignment of amino acid sequences of ECL-2 and flanking regions in human CC-chemokine receptors is shown. The alignment was made in ICM (Molsoft), and the zero end-gap global alignment algorithm was used (58). *Black background* highlights 100% conservation of a single amino acid. *Gray background* denotes ≥70% conservation of similar amino acids (in this case Tyr, Phe, and Trp). The three aromatic amino acids just C-terminal to the conserved cysteine in CCR8 are highlighted with *black boxes*. The schematic illustration in the *left panel* illustrates the area included in the alignment.

agonists acted independently of Tyr^{184}; Fig. 5*D*). Tyr^{187} was found to be essential for the action of the chemokine antagonist MC148 (Fig. 6*C*) and of minor importance for small molecule antagonism (Fig. 6*F*). To investigate whether this differential importance is matched by similar impairments of chemokine binding, homologous competition binding studies were performed. Indeed, the impaired action of CCL1 on Y184A was reflected in the binding, because no specific binding was observed of ^{125}I-CCL1 to Y184A (Fig. 7*A*). Similarly, the 12-fold decrease in potency on F186A (Fig. 5*B* and Table 1) was matched with a 4-fold decreased affinity compared with WT (13 nM compared with 3.4 nM, p = 0.032) (Fig. 7*B*) and, as expected, ^{125}I-CCL1 bound to Y187A with unaltered WT-like affinity (Fig. 7*C*). Binding of the antagonist also reflected the functional data, as ^{125}I-MC148 binding to Y187A, in marked contrast to that of ^{125}I-CCL1, was totally abolished (Fig. 7*F*). In contrast to the lack of ^{125}I-CCL1 binding to Y184A, MC148 bound to this mutant with an affinity (IC_{50}) of 14 nM (Fig. 7*D*). That is a 22-fold shift compared with the WT affinity (0.66 nM, p = 0.00004), and it matches the inhibitory potency (EC_{50}) of 4.6 nM. MC148 bound to F186A with an affinity not significantly different from the WT (1.8 nM, p = 0.098) (Fig. 7*E*). Thus, impaired chemokine binding seems to explain the lack of function for both aromatic residues in ECL-2b, with Tyr^{184} (Cys + 1) being essential for CCL1 and Tyr^{187} (Cys + 4) for MC148 binding.

Aromatic Side Chains Are Needed at Positions Cys + 1 and Cys + 4 for Chemokine Actions—To test whether the hydroxyl groups in the tyrosine residues at positions Cys + 1 and Cys + 4 have any role in chemokine interactions, both were mutated to phenylalanine, generating Y184F and Y187F, respectively. CCL1 (and the small molecule agonists ZnPhe and ZnBip) activated Y184F with WT-like potencies (Table 1), and there was no significant difference between the potencies of the MC148-mediated antagonism on this mutant compared with the WT (EC_{50} of 8.4 nM compared with 14 nM, p = 0.35). Similarly, CCL1 (and ZnPhe and ZnBip) activated Y187F with WT-like potencies (Table 1), and there was no significant difference in inhibition by MC148 compared with the WT (14 nM, p = 0.99). These data suggest that an aromatic residue, but not tyrosine specifically, is needed at positions Cys + 1 and Cys + 4 for chemokine actions.

Aromatic Residues in TMIV and TMV Play a Role in Ligand Interactions with CCR8—To gain a better understanding of the molecular environment of the aromatic residues in ECL-2b, we constructed a dynamic homology model of CCR8 based on the crystal structure of CCR5 (16) (Fig. 8*A*). Our model predicts that aromatic amino acids at positions 4.63/IV:23 and 5.34/V:−01 (Phe^{171} and Trp^{194} in CCR8, respectively) participate in direct stacking interactions with Tyr^{187}, thereby forming an aromatic cluster (Fig. 8*A*) (note that we use the nomenclature

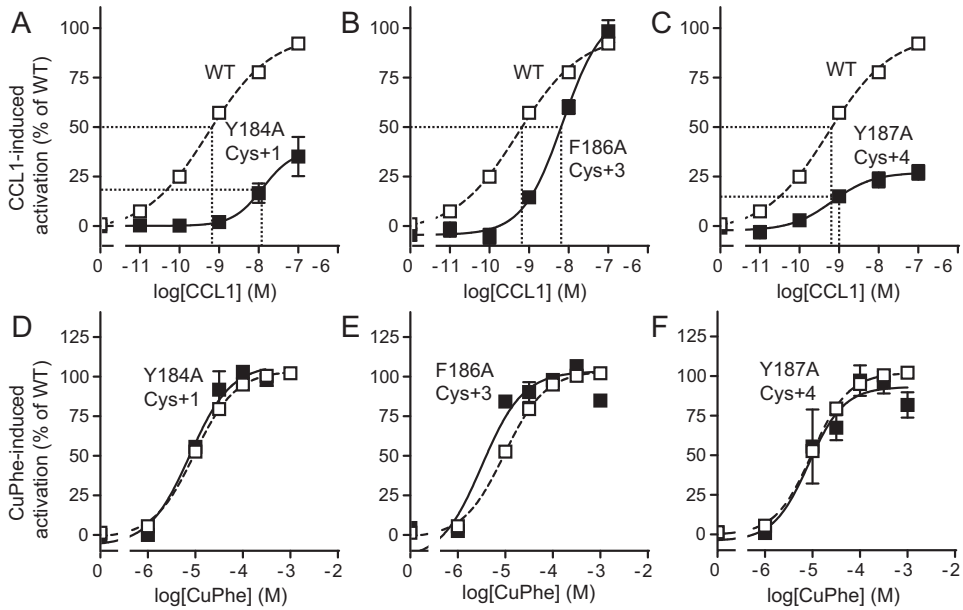

FIGURE 5. **Importance of selected aromatic amino acids in extracellular loop 2 for chemokine- and small molecule-induced activation of CCR8.** IP_3 accumulation experiments in transiently transfected COS-7 cells are shown. *A–F*, CCL1-induced (*A–C*) or CuPhe-induced (*D–F*) activation of CCR8 mutants Y184A (*A* and *D*), F186A (*B* and *E*), or Y187A (*C* and *F*). The data were normalized to WT activation (shown with a *dotted line*). The average maximal count for the CCL1-induced activation of the WT (100%) was 4151 ± 1705 cpm, and the average count for the empty vector (0%) was 1247 ± 335 cpm. For the CuPhe-induced activation, the average maximal count for the WT was 4527 ± 153 cpm, and the average count for the empty vector was 867 ± 198 cpm. The *error bars* represent S.E. ($n = 3–4$ for the mutants and $n = 20–28$ for the WT). In *A–C*, *vertical dotted lines* indicate the approximate EC_{50} values.

proposed by Ballesteros and Weinstein (36) followed by the numbering according to Baldwin and Schwartz (37, 38)). We speculated that the important role of Tyr^{187} in ligand interactions could depend upon its participation in this cluster. To test this, we mutated Phe^{171} and Trp^{194} to alanine. The F171A mutant was expressed on the cell surface at 76 ± 5% of WT level and the W194A mutant at 13 ± 4% of the WT level (Fig. 8, *B–D*).

The F171A mutation did not seem to affect the potency of CCL1 (EC_{50} of 0.29 nM compared with 0.40 nM, $p = 0.57$) (Fig. 9*A*). However, the antagonistic effect of MC148 (which is highly dependent on Tyr^{187}; Fig. 6*C*) was inhibited in this mutant (Fig. 9*B*). In the W194A mutant, neither CCL1 (Fig. 9*C*) nor the small molecule ZnPhe (Fig. 9*D*) were able to activate the receptor. For that reason, it was not possible to test the antagonistic action of MC148 in this mutant. Supporting the functional data, it was found that CCL1, but not MC148, bound to the F171A mutant (Fig. 9, *E* and *F*). Regarding the W194A mutant, although the difference in cpm values of CCL1 binding in the absence and presence of competing ligand failed to reach significance (893 ± 230 cpm compared with 394 ± 66 cpm, $p = 0.07$; Fig. 9*E*), this ligand may still bind to the mutant receptor. In contrast, there was no difference between the binding of MC148 to the W194A mutant in the absence compared with in the presence of competing ligand (144 ± 18 cpm compared with 131 ± 19 cpm, $p = 0.31$; Fig. 9*F*), suggesting that MC148 is not able to bind to W194A. In conclusion, Phe^{171} and Trp^{194} seem to be required for both binding and action of MC148 in CCR8. On the other hand, both Phe^{171} and Trp^{194} appear dispensable for the binding of CCL1 to CCR8, although Trp^{194} was required for activation by CCL1 (and by small molecule agonist).

Discussion

In this paper, we study the role of extracellular receptor regions in CCR8. Because most chemokines mainly interact with extracellular receptor parts, it is important to understand the molecular requirements for chemokine binding and actions, knowledge that in turn will improve the design of novel drugs targeting chemokine receptors. We find that although the 7TM bridge between TMIII and ECL-2 is crucial for binding and action of chemokine and small molecule ligands to and on CCR8, the CKR bridge between the N terminus and TMVII is mainly important for binding of chemokines. In addition, the binding of two different chemokines, CCL1 and MC148, depends upon distinct single aromatic residues in ECL-2: Tyr^{184} and Tyr^{187}, respectively. Homology modeling suggests that Tyr^{187} is part of an aromatic cluster between ECL-2 and Phe^{171} and Trp^{194} in TMIV and TMV, respectively, which we confirm by mutational analyses.

Importance of Conserved Disulfide Bridges for Ligand Binding and Receptor Activation—The 7TM bridge was found to be crucial for both binding and activation by all tested ligands (Figs. 1–3). In addition, the surface expression of the two 7TM bridge mutants was markedly reduced (Fig. 1, *B* and *D*); however, it was not reduced enough to explain the totally abolished ligand binding. In contrast, whereas the CKR bridge was found to be essential for chemokine binding and activation, it was dispensable for activation by small molecules (Figs. 1–3). This suggests that the CKR bridge is mainly important for ensuring correct folding of the extracellular receptor parts, which are involved in the initial binding of chemokine ligands, whereas the 7TM bridge may have a more fundamental function. Our findings confirm a recent *in silico* study of CCR8, which pre-

TABLE 1

Activation of CCR8 WT and mutants by CCL1 and small molecule agonists

IP_3 accumulation experiments in transiently transfected COS-7 cells. Potencies of CCL1- and small molecule-induced activation of receptor mutants are reported as $\log(EC_{50})$ and EC_{50}. Fold change expresses the change in EC_{50} value as compared with the WT value for each mutant. Receptor surface expression, as determined by ELISA, is reported for each mutant as a percentage of the WT expression. For Y184F and Y187F mutants, the average A_{450} was 0.255 ± 0.003 for CCR8 WT (100%) and 0.137 ± 0.0008 for the empty vector (0%). For Y184A, F186A, and Y187A mutants, the average A_{450} for the WT was 0.302 ± 0.041 and 0.135 ± 0.02 for the empty vector. *n* is the number of experiments. A significant ($p < 0.05$) difference between the EC_{50} values of a mutant receptor and the WT is highlighted in bold. ND, not determined.

	CCL1				CuBip				ZnBip				CuPhe				ZnPhe				Surface expression	
	EC_{50} ± S.E.	EC_{50}	Fold change	*n*	EC_{50} ± S.E.	EC_{50}	Fold change	*n*	EC_{50} ± S.E.	EC_{50}	Fold change	*n*	EC_{50} ± S.E.	EC_{50}	Fold change	*n*	EC_{50} ± S.E.	EC_{50}	Fold change	*n*	Mean ± S.E.	*n*
CCR8	*log*	*nM*			*log*	*μM*			*log*	*μM*			*log*	*μM*			*log*	*μM*			*% of WT*	
WT	−9.40 ± 0.13	0.40	1.0	19	−4.62 ± 0.09	24	1.0	7	−4.47 ± 0.10	34	1.0	5	−5.02 ± 0.02	9.6	1.0	20	−5.37 ± 0.13	4.3	1.0	7	100 ± 0.0	19
Y184A	−7.85 ± 0.05	14	**36**[a]	5	−4.45 ± 0.10	35	1.5	3	−4.24 ± 0.15	58	1.7	3	−5.11 ± 0.11	7.8	0.8	3	−5.49 ± 0.13	3.2	0.8	3	70 ± 10	3
Y184F	−9.86 ± 0.27	0.14	0.35	7	ND				−4.22 ± 0.11	60	1.8	3	ND				−5.18 ± 0.10	6.6	1.5	3	95 ± 12	10
F186A	−8.33 ± 0.21	4.7	**12**[b]	7	−4.55 ± 0.07	28	1.2	3	−4.28 ± 0.20	52	1.5	3	−5.49 ± 0.15	3.2	0.3	3	−5.13 ± 0.07	7.4	1.7	3	102 ± 7.7	3
Y187A	−9.07 ± 0.16	0.85	2.1	10	−4.87 ± 0.05	13	0.6	3	−4.26 ± 0.25	55	1.6	4	−5.08 ± 0.23	8.3	0.9	3	−5.03 ± 0.44	9.3	2.2	3	52 ± 7.0	3
Y187F	−9.74 ± 0.23	0.18	0.46	7	ND				−4.19 ± 0.03	65	1.9	3	ND				−5.39 ± 0.21	4.1	1.0	3	77 ± 7.5	9

[a] $p = 0.0000042$.

[b] $p = 0.00021$.

dicts the involvement of the 7TM bridge in binding of both peptide and non-peptide ligands (39). Each bridge has been shown to be required for chemokine binding to other chemokine receptors, including CCR5 (40), CXCR2 (41), and CXCR1 (42). In CCR6, on the other hand, only the 7TM bridge was essential for chemokine binding (43). However, in these studies, small molecule-induced activation (and thereby the ability of the mutant receptors to be activated independently of chemokine binding) was not tested. We recently reported that the disulfide bridges play different roles in the receptors CCR1 and CCR5 (44). In CCR1, the 7TM bridge was found to be essential for activation with both chemokine and small molecule ligands, whereas the CKR bridge was not required for small molecule-mediated activation. However, in contrast to our findings for CCR8 and to studies of other receptors, high affinity chemokine binding to CCR1 was retained after breaking either bridge. For CCR5, chemokine binding and activation depended on both bridges, whereas activation with small molecules was independent on either bridge. Thereby, the three closely related receptors CCR1, CCR5, and CCR8 have very different dependences on the two bridges despite an overlap in small molecule and chemokine ligands (31).

Roles of Aromatic Amino Acids in ECL-2—In CC-chemokine receptors, aromatic residues are conserved in ECL-2 at position Cys + 4 (Fig. 4*B*). Regarding the class A 7TM receptor family as a whole, the degree of conservation of aromatic residues at position Cys + 4 is not accurately determined because of alignment uncertainties in ECL-2. However, when looking at the currently available crystal structures of class A 7TM receptors, 11 of 20 human receptors (including two chemokine receptors) have an aromatic residue in position Cys + 4. In 9 of those 11 receptors, the aromatic residue is positioned in the interface between TMIV and TMV with the aromatic ring pointing down into the main binding pocket (Fig. 10*A*). Furthermore, in several of the class A crystal structures, aromatic residues in ECL-2 are predicted to interact directly with the bound ligands (10–12, 45). In CCR8 we observed that two of the three aromatic residues in ECL-2b were crucial for chemokine binding, because CCL1 depended on Tyr^{184} (Cys + 1), and Tyr^{187} (Cys + 4) was essential for MC148 (9) (Fig. 7). In a study of CCR1, the phenylalanine in position Cys + 4 was found to be important for the activation of the receptor by both chemokine and small molecule agonists (9). Furthermore, alanine mutation of the tyrosine in position Cys + 1 in CXCR1 resulted in markedly reduced binding of its chemokine ligand CXCL8 (42). Together with the present study, these findings confirm the predicted involvement of aromatic residues in ECL-2 in ligand binding and receptor activation. Furthermore, our study confirms the prediction by the aforementioned *in silico* study that Tyr^{184} is involved in ligand interactions in CCR8 (39).

Presence of an Aromatic Cluster in the Top of the Ligand Binding Pocket in Chemokine Receptors—No crystal structure is available of CCR8, but crystal structures are present of the two human chemokine receptors CCR5 (16) and CXCR4 (13, 17) and of the viral chemokine receptor US28 (47). Homology modeling can be a useful tool to obtain tertiary structural information for receptors for which crystal structures are not available. From our homology model of CCR8, we predicted that Tyr^{187}

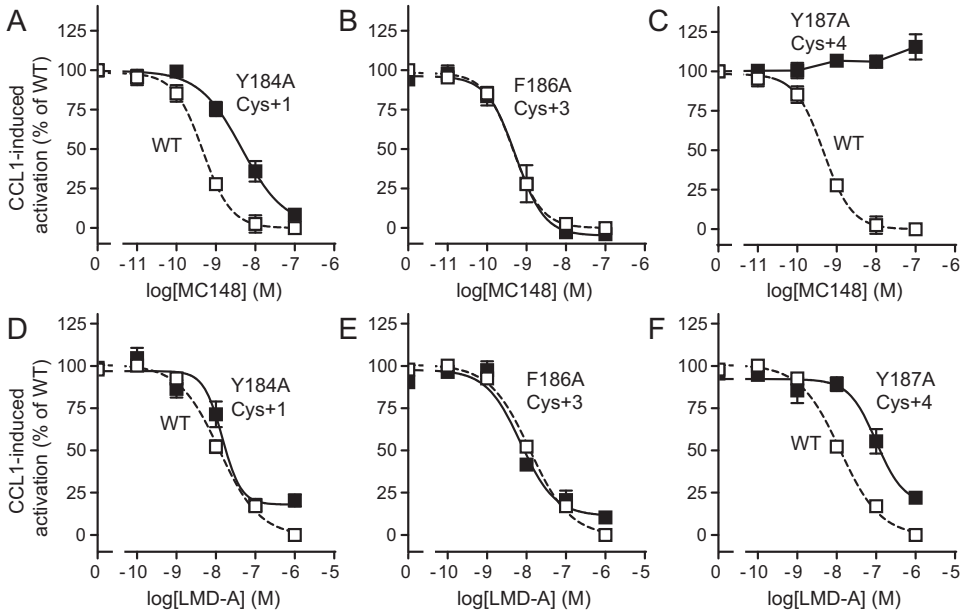

FIGURE 6. **Importance of selected aromatic amino acids in extracellular loop 2 for chemokine- and small molecule-mediated antagonism on CCR8.** IP_3 accumulation experiments in transiently transfected COS-7 cells are shown. *A–F*, MC148-mediated (*A–C*) or LMD-A-mediated (*D–F*) antagonism of CCL1-induced activation of CCR8 mutants Y184A (*A* and *D*), F186A (*B* and *E*), or Y187A (*C* and *F*). WT activation is illustrated with a *dotted line*. The data were normalized to WT activation. The average maximal count for the CCL1-induced activation of the WT (100%) was 4151 ± 1705 cpm, and the average count for the empty vector (0%) was 1247 ± 335 cpm. For the CuPhe-induced activation, the average maximal count for the WT was 4527 ± 153 cpm, and the average count for the empty vector was 867 ± 198 cpm. The *error bars* represent S.E. ($n = 3$ for the mutants and $n = 4–7$ for the WT).

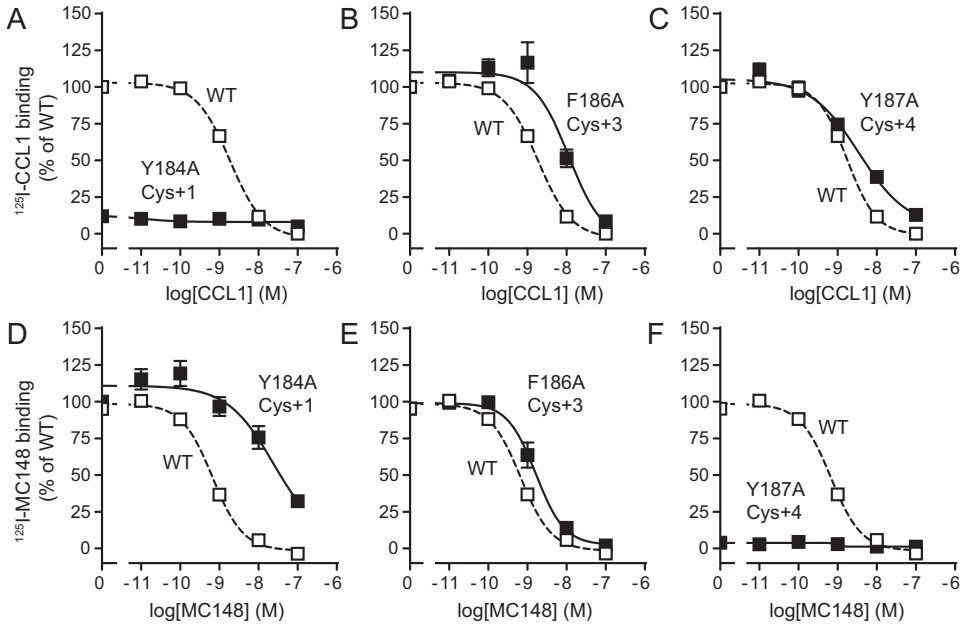

FIGURE 7. **Dependence of CC-chemokine binding on selected aromatic residues in extracellular loop 2 of CCR8.** *A–F*, homologous competition binding using ^{125}I-CCL1 (*A–C*) and ^{125}I-MC148 (*D–F*) in transiently transfected COS-7 cells expressing Y184A (*A* and *D*), F186A (*B* and *E*), or Y187A (*C* and *F*). The data were normalized to WT binding, which is illustrated with a *dotted line*. In ^{125}I-CCL1 binding experiments, the maximal average value for the WT receptor was 1970 ± 103 cpm, and the average count for the empty vector was 625 ± 109 cpm. In ^{125}I-MC148 binding experiments, the maximal average value for the WT receptor was 463 ± 127 cpm, and the average count for the empty vector was 31 ± 10 cpm. The *error bars* represent S.E. ($n = 3–9$).

interacts with aromatic residues at positions 4.63/IV:23 and 5.34/V:−01 in the flanking TM domains (Fig. 8*A*), which we confirmed by *in vitro* mutagenesis studies (Fig. 9). Interestingly, aromatic residues are overrepresented at these positions in the family of CC-chemokine receptors (Fig. 4). At position 4.63/IV:23, an aromatic residue is found in all 10 receptors and at position 5.34/V:−01, 7 of 10 receptors have a tryptophan, and 1 receptor has a phenylalanine. For class A 7TM receptors in general, the degree of structural conservation in these positions is not clear, because the large variation in helix lengths makes an alignment of these regions close to ECL-2 too hypothetical. When comparing our CCR8 homology model with the available crystal structures of chemokine receptors, we see that in both CCR5 and CXCR4, the aromatic residue in position Cys + 4 participates in stacking interactions with aromatic residues at positions 4.63/IV:23 and 5.34/V:−01. These residues form aro-

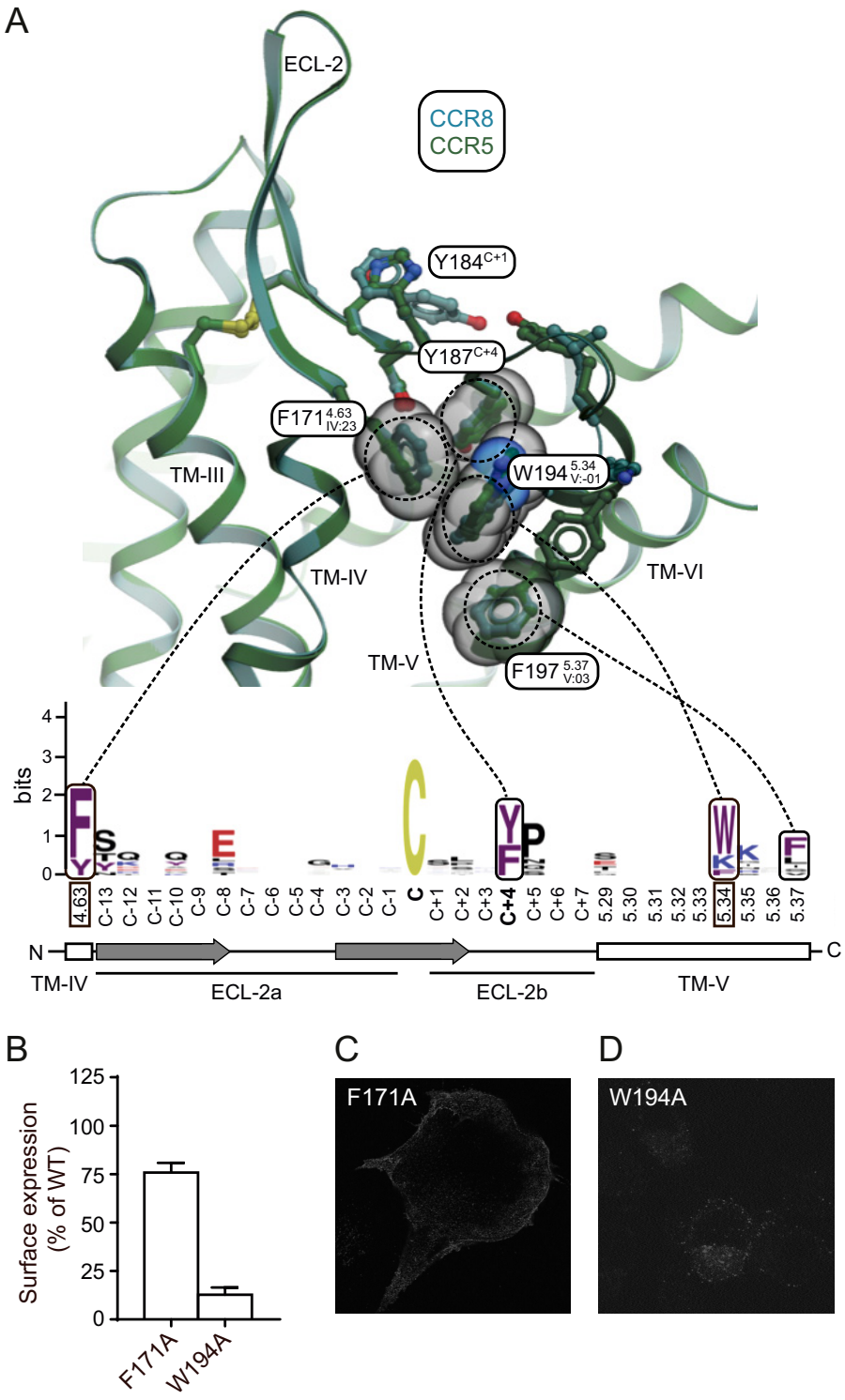

FIGURE 8. **Involvement of aromatic residues in the top of transmembrane helices IV and V in a putative aromatic cluster in CCR8.** *A*, structural conservation of the aromatic residues at the TMIV/TMV interface in the CC-chemokine receptor subfamily. The CCR5-based homology model of CCR8 (*blue*) was superimposed onto the high resolution crystal structure of CCR5 (*green*; Protein Data Bank code 4MBS). Important side chains are shown as stick representations. The van der Waals surface is shown for aromatic ring systems of conserved residues. The amino acid conservation of the extracellular sides of TMIV/TMV and ECL-2 is shown as sequence logo for the human CC receptor subfamily (CCR1–10). The logo displays the frequencies of amino acids on each position as the relative heights of letters, along with the degree of sequence conservation as the total height of a stack of letters, measured in bits of information. Secondary structure elements are shown as *white boxes* (α-helix) and *gray arrows* (β-sheet). Two of the positions where aromatic residues are conserved, 4.63 (Phe^{171} in CCR8) and 5.34 (Trp^{194} in CCR8), are highlighted with *black boxes*. The figure was made using ICM (59). *B–D*, surface expression of aromatic amino acid mutants F171A and W194A. *B*, ELISA on COS-7 cells transiently transfected with each mutant receptor ($n = 7–11$). The surface expression is shown as a percentage of WT receptor surface expression (100%, average $A_{450} = 0.214 \pm 0.02$). The average empty vector value (0%) was 0.168 ± 0.021. *C* and *D*, representative confocal microscopy pictures of COS-7 cells transiently transfected with F171A (*C*) or W194A (*D*).

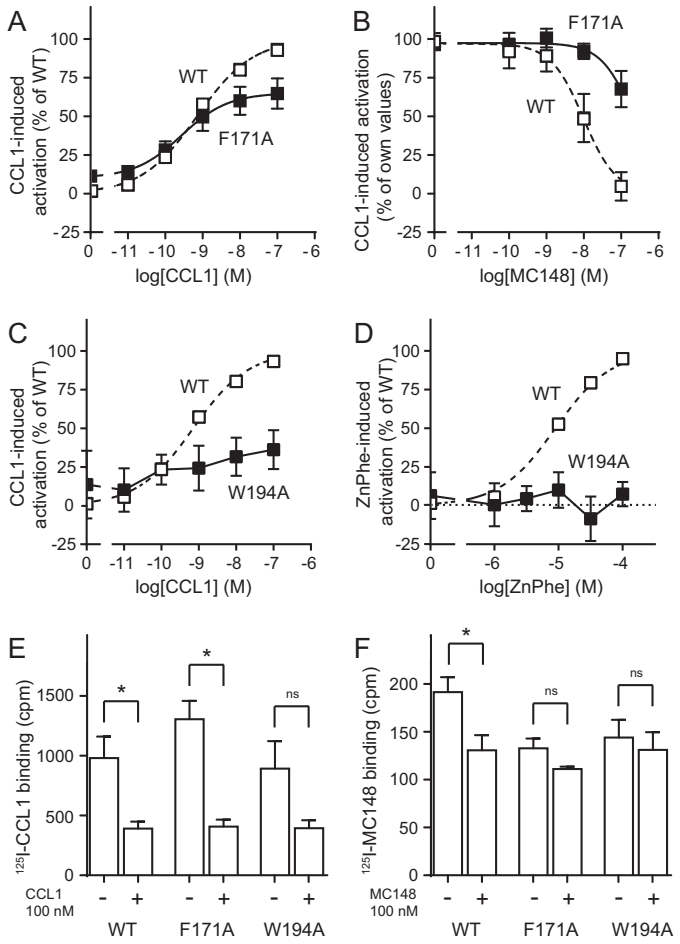

FIGURE 9. **Role of selected aromatic amino acids in the transmembrane regions flanking extracellular loop 2 in receptor activation and binding in CCR8.** *A–D*, IP_3 accumulation experiments in transiently transfected COS-7 cells. *A*, CCL1-induced activation of F171A. *B*, MC148-mediated antagonism of CCL1-induced activation of F171A. *C* and *D*, CCL1-induced (*C*) or ZnPhe-induced (*D*) activation of W194A. The data were normalized to WT values (*A*, *C*, and *D*) or to own values (*B*). WT graphs are shown as *dotted lines* for comparison. For CCL1-mediated activation, the average maximal WT value was 1268 ± 99 cpm. For ZnPhe-mediated activation, the average maximal WT value was 655 ± 64 cpm. In *B*, the maximal value of CCL1-mediated activation of F171A, which was 849 ± 44 cpm, was used for the normalization. *Error bars* represent S.E., $n = 6–7$, except for CCL1 on the WT, where $n = 33$. *E* and *F*, homologous competition binding assays in transiently transfected COS-7 cells. The cpm values for the binding of ^{125}I-CCL1 (*E*) or ^{125}I-MC148 (*F*) to CCR8 WT, F171A, and W194A are given. Binding in the presence (+) or absence (−) of 100 nM competing cold ligand (CCL1 in *E* and MC148 in *F*) is shown for all receptor constructs ($n = 4–5$). An *asterisk* denotes a statistically significant ($p < 0.05$) difference. *ns* means that there is no statistically significant difference.

matic clusters very similar to the one in our model (Fig. 10, *B* and *C*). Likewise as in our model, the aromatic residue at position 5.37/V:03 in CCR5 also participates in the cluster but without interacting directly with the residue in Cys + 4. In CXCR4, an aromatic residue at position 5.38/V:04 plays this role. The viral chemokine receptor US28, which binds CX3C-chemokines as well as CC-chemokines (48–50), has aromatic residues both at position Cys + 4 and at position 5.34/V:−01, but it lacks an aromatic residue at position 4.63/IV:23 and does not have a tightly packed aromatic cluster like the other receptors (Fig. 10*D*). The overrepresentation of aromatic residues in ECL-2 and TMIV and TMV suggests that an aromatic cluster could be present throughout the family of endogenous CC-chemokine receptors.

Role of the Aromatic Cluster in Ligand Interactions and Receptor Activation—In class A receptors, the 7TM bridge forces ECL-2 into a conformation where it is bent toward the receptor core, forming a "lid" over the main ligand binding pocket. This ECL-2 lid has been proposed to control the activation state of the receptor, possibly by assuming different conformations in ligand-bound and ligand-free states (51–53). The important role of the aromatic cluster between ECL-2 and TMIV and TMV in ligand interactions in CCR8, reported in this study, suggests that this cluster accounts for at least some of the roles of ECL-2 in ligand interactions and receptor activation in chemokine receptors (and putatively other receptor families). It is interesting that the binding of MC148, but not of CCL1, is found to be highly dependent on all three aromatic residues of this cluster (Figs. 7, *C* and *F*, and 9, *E* and *F*), suggesting that the cluster may have ligand-specific roles.

Other aromatic clusters have been reported to play important roles in chemokine receptor activation, including a cluster between TMII and TMIII in CCR5 (54) and an aromatic zipper composed of residues in TMIII, TMVI, and TMVII in CXCR3 (55). Whether the aromatic cluster identified in this study contributes to keeping ECL-2 in a "locked" state, which supports a certain receptor conformation, requires further investigation. However, it is noteworthy that US28, which does not have this aromatic cluster, is a constitutively active receptor (56, 57).

In summary, we here demonstrate the importance of extracellular domains, and in particular ECL-2, for ligand interactions and receptor activation in CCR8. We demonstrate that different single aromatic residues in ECL-2 are required for binding of the chemokines CCL1 and MC148 and suggest the presence of an aromatic cluster between ECL-2 and TM domains IV and V of importance for ligand interactions and receptor activation in chemokine receptors in general. This study suggests that treatments could be developed that selectively target the binding of a specific chemokine to a chemokine receptor. Furthermore, it opens up for new studies of the aromatic cluster in other chemokine receptors, with the potential to give valuable information about the mechanism of chemokine receptor activation. This is expected to lead to the development of new drugs targeting this family of receptors.

Experimental Procedures

Materials—Human CCL1 was purchased from Peprotech (Rocky Hill, NJ). The plasmid encoding the viral ligand MC148 was kindly provided by Hans Lüttichau (University of Copenhagen, Copenhagen, Denmark), and the protein was expressed and purified as described below. [^{125}I]CCL1 (100T Bq·mmol^{-1}) was either purchased from PerkinElmer or prepared in house. [^{125}I]MC148 (~100T Bq·mmol^{-1}) was prepared in house. Small molecule agonists were purchased from Sigma-Aldrich, and LMD-A was kindly provided by Roland Kolbeck, Millennium Pharmaceuticals (Cambridge, MA). The human *ccr8* WT cDNA was kindly provided by Tim Wells (Serono Pharmaceutical Research Institute, Geneva, Switzerland). *myo*-[^{3}H]Inositol (PT6–271) was purchased from Amersham Biosciences,

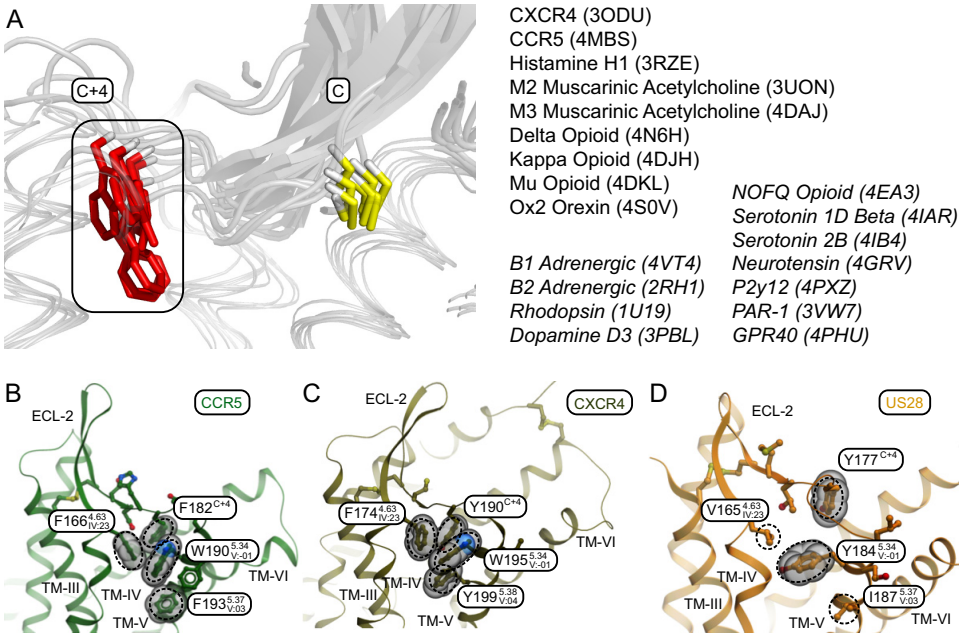

FIGURE 10. **Structure of the TMIV/TMV aromatic interface in available crystal structures of class A 7TM receptors.** *A*, structural arrangement of the aromatic amino acid at position Cys + 4 (in *red*) in nine crystal structures of class A 7TM receptors. The conserved cysteine is shown in *yellow*. The names of the nine receptors are listed in the top list to the *right*. The receptors written below in *italics* either do not have an aromatic residue in Cys + 4 (10 receptors) or their aromatic residue is differently arranged (GPR40 and rhodopsin). *B*, the human receptor CCR5 (Protein Data Bank code 4MBS). *C*, the human receptor CXCR4 (Protein Data Bank code 4RWS). *D*, the cytomegalovirus receptor US28 (Protein Data Bank code 4XT1). Important side chains are shown as stick representation. The van der Waals surface is shown for aromatic ring systems of selected receptor residues. *A* was made in PyMOL, and *B–D* were made using ICM (59).

and the chimeric G protein $G\alpha_{\Delta 6qi4myr}$ was kindly provided by Evi Kostenis (University of Bonn, Bonn, Germany).

Site-directed Mutagenesis—Mutations were generated with the PCR overlap extension technique with human *ccr8* WT as template, using the *Pfu* polymerase (Stratagene, Santa Clara, CA). The constructs were cloned into the eukaryotic expression vector pcDNA3.1, and the mutations were verified by DNA sequencing.

Tissue Culture—COS-7 cells (LGC/ATCC, Teddington, Middlesex, UK) were grown at 37 °C and 10% CO_2 in Dulbecco's modified Eagle's medium with GlutaMAX (Gibco; cat. no. 21885-025) supplemented with 10% FBS, 180 $\mu g \cdot ml^{-1}$ penicillin and 45 $\mu g \cdot ml^{-1}$ streptomycin.

Purification of MC148—Expression and purification of MC148 was performed as previously described (25); COS-7 cells were transfected as described above and kept in serum-free medium, which was collected 24, 48, and 56 h post-transfection and adjusted to pH 4.5. It was centrifuged at 1500 × *g* for 20 min at room temperature, and the supernatant was filtered through a 0.22-μm filter and diluted 1:1 with sterilized water. The samples were loaded onto cation SP-Sepharose fast flow columns (Pharmacia Biotech), which were washed with 50 mM acetate buffer, pH 4.5. The protein was eluted with 2 M NaCl in the same buffer. The eluate was made 0.2% in TFA, filtered, and loaded on a C8 column (Vydac) for reverse phase HPLC. The protein was eluted from the C8 column with 0.1% TFA in water on a gradient of acetonitrile. The purity of MC148 was assessed by mass spectrometry and N-terminal sequencing on an ABI 494 protein sequencer (PerkinElmer).

Inositol Phosphate Assay—COS-7 cells were transfected by the calcium phosphate precipitation method (60) as described previously (28). For 75-cm^2 flasks, plasmid DNA was mixed with 30 μl of 2 mM $CaCl_2$ and TE buffer (10 mM Tris-HCl, 1 mM EDTA, pH 7.4) to a final volume of 240 μl. An equal volume of 2× HBS buffer (280 mM NaCl, 50 mM HEPES, 1.5 mM Na_2HPO_4, pH 7.2) was added, and the mixture was incubated at room temperature for 45 min, before it was added to the cells with 150 μl of 2 $mg \cdot ml^{-1}$ chloroquine in 5 ml of cell culture medium. After 5 h at 37 °C, the medium was replaced with fresh medium. In this assay, the cells were co-transfected with the chimeric G protein $G\alpha_{\Delta 6qi4myr}$, which turns the signal from $G\alpha_i$-coupled receptors into a $G\alpha_q$ response (61). Using this approach, the activity of a $G\alpha_i$-coupled receptor (like endogenous chemokine receptors) can be measured with a read-out for $G\alpha_q$ activity—in this case phosphatidylinositol bisphosphate turnover—without alterations in the intracellular receptor regions (61). In other words, this is a method where a signal transduction pathway is "directed" in a certain manner ($G\alpha_i$ to $G\alpha_q$) without interference with the receptor structure, but only by interference with the G protein downstream of the receptor.

For a 75-cm^2 flask, 10 μg of receptor DNA and 15 μg of $G\alpha_{\Delta 6qi4myr}$ was used. The generated inositol trisphosphate was measured using one of two strategies, which have been shown to give the same results, as described before (31). Using the first strategy, cells were seeded in 24-well plates ($1.5 \cdot 10^5$ cells per well) 1 day after transfection and incubated with 7.5 μCi of *myo*-[^{3}H]inositol in 0.3 ml of growth medium for 24 h. After two washes with PBS, ligands were added in 0.2 ml of Hank's balanced salt solution (Invitrogen) supplemented with 10 mM LiCl, and the cells were incubated at 37 °C for 90 min. When used, antagonists were added 10 min prior to the agonists. After medium removal, the cells were extracted by adding 1 ml of 10 mM formic acid to each well and incubating on ice for 30–60 min. The generated [^{3}H]inositol phosphate was purified on an

AG 1-X8 anion exchange resin from Bio-Rad. Multipurpose liquid scintillation mixture (Gold Star, Triskem-International, Bruz, France) was added, and radiation was counted in a Beckman Coulter counter LS6500 (Beckman Coulter Danmark ApS c/o OptiNordic ApS, Copenhagen, Denmark). Using the second measurement strategy, the cells were seeded in 96-well plates (3.5×10^4 cells/well) and incubated with 25 μCi of *myo*-[^{3}H]inositol/ml growth medium in 100 μl for 24 h. The cells were then incubated with ligands and extracted as described above, only with different volumes: 100 μl of ligand solution with LiCl and 50 μl of formic acid. 20 μl of the extract was transferred to a 96-well plate and mixed with 80 μl of a 1:8 dilution of YSi poly-D-lysine coated scintillation proximity assay beads (PerkinElmer) in water. The plates were agitated for at least 30 min and centrifuged (5 min, 400 $\times$ *g*). Scintillation was determined using a Packard Top Count NXT^{TM} scintillation counter (PerkinElmer). Determinations were made in duplicate. Unspecific activity was defined as the activity in mock-transfected cells. GraphPad prism software was used, and the EC_{50} values were calculated by non-linear regression, according to Equation 1, where y is the measured activity, x is the concentration of ligand, and N is the average background activity (the activity in mock-transfected cells).

$$y = N + \frac{(T - N)}{1 + 10^{\log(EC_{50} - x)}} \quad \text{(Eq. 1)}$$

Homologous Competition Binding Assay—COS-7 cells were transfected using the calcium phosphate transfection protocol, as described above. 20 μg of receptor DNA was used for a 75-cm^2 flask. The following day, the transfected cells were seeded in culture plates. The assay was performed as described earlier (28). The number of cells seeded per well was determined from the apparent efficiencies of receptor expression and aimed at obtaining 5–10% specific binding of the radioligand (1×10^4 to 15×10^4 cells/well). Two days after transfection, the cells were incubated with 10–15 pM labeled ligand and different concentrations of unlabeled ligand, in 0.2 ml of 50 mM HEPES buffer (pH 7.4, supplemented with 1 mM $CaCl_2$, 5 mM $MgCl_2$ and 0.5% (w/v) BSA) at 4 °C for 3 h. The cells were washed twice in the same buffer supplemented with 0.5 M NaCl, lysed, and the radiation was counted using a Wallac gamma counter. Determinations were made in duplicate. The data were analyzed using GraphPad prism software. The program calculated IC_{50} values using non-linear regression according to Equation 2. In this case, x is the concentration of labeled ligand, and the other factors are as described for Equation 1. According to the equation by Cheng and Prusoff (62) (Equation 3), in a homologous competition binding experiment where the concentration of labeled ligand is only a small fraction of the IC_{50} value (<3%), $K_d \approx IC_{50}$, and the affinity can therefore be expressed as an IC_{50} value.

$$y = N + \frac{(T - N)}{1 + 10^{\log(x) - \log(IC_{50})}} \quad \text{(Eq. 2)}$$

$$K_d = IC_{50} - x \quad \text{(Eq. 3)}$$

Cell Surface Expression by ELISA—COS-7 cells were transfected with N-terminally FLAG-tagged *ccr8* constructs using one of two procedures: the calcium phosphate precipitation procedure or the Lipofectamine procedure. Using the calcium phosphate transfection protocol (used for the aromatic amino acid mutants in parallel with CCR8 WT), the cells were transfected as described above with 10 μg of receptor DNA for a 25-cm^2 flask and the following day were seeded out, 3.5×10^4 cells/well, in 96-well plates. Using the Lipofectamine protocol (used for the disulfide bridge mutants in parallel with CCR8 WT), the cells were transfected directly in the wells using Lipofectamine (Invitrogen), according to the manufacturer's instructions. The following day, the assay was performed as described earlier (9). The cells were washed in TBS buffer (50 mM Tris-base, 150 mM NaCl, 1 mM $CaCl_2$, pH 7.6) and fixed for 10 min in 150 μl of 4% formaldehyde. Then cells were washed three times, blocked in TBS with 2% BSA for 30 min, and incubated for 90 min with 2 $\mu g \cdot ml^{-1}$ mouse M1 anti-FLAG antibody (Sigma) in TBS with 2% BSA. Following three washes with TBS, the cells were incubated for 1 h with horseradish peroxidase-conjugated goat anti-mouse IgG antibody (Pierce) diluted 1:1000 in TBS containing 2% BSA. After three washes, the assay was developed by addition of horseradish peroxidase substrate, according to the manufacturer's recommendations.

Confocal Microscopy—COS-7 cells were transfected with N-terminally FLAG-tagged *ccr8* constructs using the calcium phosphate transfection protocol, as described above. 10 μg of receptor DNA was used for a 25-cm^2 flask. 24 h later, the transfected cells were seeded on 12-mm round coverslips, 7.0×10^4 cells/coverslip. Next day, the cells were fixed in 4% paraformaldehyde for 15 min, washed three times with TBS, and then blocked in TBS with 2% BSA for 30 min. The cells were then incubated with 2 $\mu g \cdot ml^{-1}$ mouse M1 anti-FLAG antibody (Sigma) in TBS with 2% BSA for 90 min at room temperature. Following three washes with TBS, the cells were then incubated for 1 h with goat anti-mouse Alexa Fluor 568-conjugated IgG antibody (Invitrogen, Molecular Probes), diluted 1:500 in TBS with 2% BSA. The cells were washed three times, and the slides were mounted. Pictures were taken with a Zeiss LSM-780 laser scanning confocal microscope using a 63× oil NA 1.40 objective.

Molecular Modeling—Homology modeling of CCR8 was performed using "Internal Coordinate Mechanics" (Molsoft, San Diego, CA). The structure of the closely related hCCR5 receptor (Protein Data Bank code 4MBS; 41% sequence identity to hCCR8), solved to 2.7 Å resolution, was obtained from the RCSB Protein Data Bank, and used as template. Crystallization water and co-crystallized molecules were deleted, and the structure was converted to an ICM object, thereby assigning protein atom types, optimizing hydrogens and His, Pro, Asn, Gly, and Cys side chain conformations. The receptor model was subjected to 300 steps of Cartesian minimization and 200 steps of global side chain minimization to yield a structure in a low energy conformation. Alignments were based on the zero end-gap global alignment algorithm (63). Sequence logos were generated using WebLogo 3 (46, 64). Sequences of the human CC receptor family were obtained from UniProt.

Statistical Analysis—Statistical analysis was performed in Excel. Analysis of significance was carried out using the unpaired two-tailed *t* test. A *p* value of less than 0.05 was considered statistically significant.

Author Contributions—L. B. conducted some of the experiments, analyzed the data, and wrote the manuscript. P. C. R. designed the research study, conducted some of the experiments, analyzed the data, and wrote the manuscript. M. L. performed the molecular modelling of CCR8. H. P. conducted some of the experiments and analyzed the data. O. L. iodinated proteins and analyzed the data. V. D. performed the microscopy and analyzed the data. A. H. J. performed the mass spectrometry and analyzed the data. T. M. F. analyzed the structural conservation of the aromatic cluster in different receptors. S. K. conducted some of the experiments and analyzed the data. M. M. R. designed the research study, analyzed the data, and wrote the manuscript.

Acknowledgments—We thank Maibritt Sigvardt Baggesen and Lisbet Elbak for skillful technical assistance.

References

1. Gerard, C., and Rollins, B. J. (2001) Chemokines and disease. *Nat. Immunol.* **2,** 108–115
2. Rosenkilde, M. M., and Schwartz, T. W. (2004) The chemokine system: a major regulator of angiogenesis in health and disease. *APMIS* **112,** 481–495
3. Viola, A., and Luster, A. D. (2008) Chemokines and their receptors: drug targets in immunity and inflammation. *Annu. Rev. Pharmacol. Toxicol.* **48,** 171–197
4. Schwarz, M. K., and Wells, T. N. (2002) New therapeutics that modulate chemokine networks. *Nat. Rev. Drug Discov.* **1,** 347–358
5. Allen, S. J., Crown, S. E., and Handel, T. M. (2007) Chemokine: receptor structure, interactions, and antagonism. *Annu. Rev. Immunol.* **25,** 787–820
6. Thiele, S., and Rosenkilde, M. M. (2014) Interaction of chemokines with their receptors: from initial chemokine binding to receptor activating steps. *Curr. Med. Chem.* **21,** 3594–3614
7. Rosenkilde, M. M., Benned-Jensen, T., Frimurer, T. M., and Schwartz, T. W. (2010) The minor binding pocket: a major player in 7TM receptor activation. *Trends Pharmacol. Sci.* **31,** 567–574
8. Rosenkilde, M. M., and Schwartz, T. W. (2006) GluVII:06: a highly conserved and selective anchor point for non-peptide ligands in chemokine receptors. *Curr. Top. Med. Chem.* **6,** 1319–1333
9. Jensen, P. C., Thiele, S., Steen, A., Elder, A., Kolbeck, R., Ghosh, S., Frimurer, T. M., and Rosenkilde, M. M. (2012) Reversed binding of a small molecule ligand in homologous chemokine receptors: differential role of extracellular loop 2. *Br. J. Pharmacol.* **166,** 258–275
10. Warne, T., Serrano-Vega, M. J., Baker, J. G., Moukhametzianov, R., Edwards, P. C., Henderson, R., Leslie, A. G., Tate, C. G., and Schertler, G. F. (2008) Structure of a β1-adrenergic G-protein-coupled receptor. *Nature* **454,** 486–491
11. Jaakola, V. P., Griffith, M. T., Hanson, M. A., Cherezov, V., Chien, E. Y., Lane, J. R., Ijzerman, A. P., and Stevens, R. C. (2008) The 2.6 angstrom crystal structure of a human A2A adenosine receptor bound to an antagonist. *Science* **322,** 1211–1217
12. Palczewski, K., Kumasaka, T., Hori, T., Behnke, C. A., Motoshima, H., Fox, B. A., Le Trong, I., Teller, D. C., Okada, T., Stenkamp, R. E., Yamamoto, M., and Miyano, M. (2000) Crystal structure of rhodopsin: a G protein-coupled receptor. *Science* **289,** 739–745
13. Wu, B., Chien, E. Y., Mol, C. D., Fenalti, G., Liu, W., Katritch, V., Abagyan, R., Brooun, A., Wells, P., Bi, F. C., Hamel, D. J., Kuhn, P., Handel, T. M., Cherezov, V., and Stevens, R. C. (2010) Structures of the CXCR4 chemokine GPCR with small-molecule and cyclic peptide antagonists. *Science* **330,** 1066–1071
14. Cherezov, V., Rosenbaum, D. M., Hanson, M. A., Rasmussen, S. G., Thian, F. S., Kobilka, T. S., Choi, H. J., Kuhn, P., Weis, W. I., Kobilka, B. K., and Stevens, R. C. (2007) High-resolution crystal structure of an engineered human β2-adrenergic G protein-coupled receptor. *Science* **318,** 1258–1265
15. Park, S. H., Das, B. B., Casagrande, F., Tian, Y., Nothnagel, H. J., Chu, M., Kiefer, H., Maier, K., De Angelis, A. A., Marassi, F. M., and Opella, S. J. (2012) Structure of the chemokine receptor CXCR1 in phospholipid bilayers. *Nature* **491,** 779–783
16. Tan, Q., Zhu, Y., Li, J., Chen, Z., Han, G. W., Kufareva, I., Li, T., Ma, L., Fenalti, G., Li, J., Zhang, W., Xie, X., Yang, H., Jiang, H., Cherezov, V., *et al.* (2013) Structure of the CCR5 chemokine receptor-HIV entry inhibitor maraviroc complex. *Science* **341,** 1387–1390
17. Qin, L., Kufareva, I., Holden, L. G., Wang, C., Zheng, Y., Zhao, C., Fenalti, G., Wu, H., Han, G. W., Cherezov, V., Abagyan, R., Stevens, R. C., and Handel, T. M. (2015) Structural biology: crystal structure of the chemokine receptor CXCR4 in complex with a viral chemokine. *Science* **347,** 1117–1122
18. Zhang, D., Gao, Z. G., Zhang, K., Kiselev, E., Crane, S., Wang, J., Paoletta, S., Yi, C., Ma, L., Zhang, W., Han, G. W., Liu, H., Cherezov, V., Katritch, V., Jiang, H., *et al.* (2015) Two disparate ligand-binding sites in the human P2Y1 receptor. *Nature* **520,** 317–321
19. Zhang, K., Zhang, J., Gao, Z. G., Zhang, D., Zhu, L., Han, G. W., Moss, S. M., Paoletta, S., Kiselev, E., Lu, W., Fenalti, G., Zhang, W., Müller, C. E., Yang, H., Jiang, H., *et al.* (2014) Structure of the human P2Y12 receptor in complex with an antithrombotic drug. *Nature* **509,** 115–118
20. Soler, D., Chapman, T. R., Poisson, L. R., Wang, L., Cote-Sierra, J., Ryan, M., McDonald, A., Badola, S., Fedyk, E., Coyle, A. J., Hodge, M. R., and Kolbeck, R. (2006) CCR8 expression identifies CD4 memory T cells enriched for FOXP3+ regulatory and Th2 effector lymphocytes. *J. Immunol.* **177,** 6940–6951
21. Pease, J. E. (2010) Is there a role for CCR8 in the pathogenesis of asthma? *Clin. Exp. Allergy* **40,** 1110–1112
22. Panina-Bordignon, P., Papi, A., Mariani, M., Di Lucia, P., Casoni, G., Bellettato, C., Buonsanti, C., Miotto, D., Mapp, C., Villa, A., Arrigoni, G., Fabbri, L. M., and Sinigaglia, F. (2001) The C-C chemokine receptors CCR4 and CCR8 identify airway T cells of allergen-challenged atopic asthmatics. *J. Clin. Invest.* **107,** 1357–1364
23. Islam, S. A., Ling, M. F., Leung, J., Shreffler, W. G., and Luster, A. D. (2013) Identification of human CCR8 as a CCL18 receptor. *J. Exp. Med.* **210,** 1889–1898
24. Damon, I., Murphy, P. M., and Moss, B. (1998) Broad spectrum chemokine antagonistic activity of a human poxvirus chemokine homolog. *Proc. Natl. Acad. Sci. U.S.A.* **95,** 6403–6407
25. Lüttichau, H. R., Stine, J., Boesen, T. P., Johnsen, A. H., Chantry, D., Gerstoft, J., and Schwartz, T. W. (2000) A highly selective CC chemokine receptor (CCR)8 antagonist encoded by the poxvirus *Molluscum contagiosum*. *J. Exp. Med.* **191,** 171–180
26. Jin, J., Wang, Y., Wang, F., Kerns, J. K., Vinader, V. M., Hancock, A. P., Lindon, M. J., Stevenson, G. I., Morrow, D. M., Rao, P., Nguyen, C., Barrett, V. J., Browning, C., Hartmann, G., Andrew, D. P., *et al.* (2007) Oxazolidinones as novel human CCR8 antagonists. *Bioorg. Med. Chem. Lett.* **17,** 1722–1725
27. Jenkins, T. J., Guan, B., Dai, M., Li, G., Lightburn, T. E., Huang, S., Freeze, B. S., Burdi, D. F., Jacutin-Porte, S., Bennett, R., Chen, W., Minor, C., Ghosh, S., Blackburn, C., Gigstad, K. M., Jones, M., *et al.* (2007) Design, synthesis, and evaluation of naphthalene-sulfonamide antagonists of human CCR8. *J. Med. Chem.* **50,** 566–584
28. Rummel, P. C., Arfelt, K. N., Baumann, L., Jenkins, T. J., Thiele, S., Lüttichau, H. R., Johnsen, A., Pease, J., Ghosh, S., Kolbeck, R., and Rosenkilde, M. M. (2012) Molecular requirements for inhibition of the chemokine receptor CCR8: probe-dependent allosteric interactions. *Br. J. Pharmacol.* **167,** 1206–1217
29. Karlsson, A. K., Walles, K., Bladh, H., Connolly, S., Skrinjar, M., and Rosendahl, A. (2011) Small molecule antagonists of CCR8 inhibit eosinophil and T cell migration. *Biochem. Biophys. Res. Commun.* **407,** 764–771
30. Jensen, P. C., Nygaard, R., Thiele, S., Elder, A., Zhu, G., Kolbeck, R., Ghosh,

S., Schwartz, T. W., and Rosenkilde, M. M. (2007) Molecular interaction of a potent nonpeptide agonist with the chemokine receptor CCR8. *Mol. Pharmacol.* **72,** 327–340
31. Thiele, S., Malmgaard-Clausen, M., Engel-Andreasen, J., Steen, A., Rummel, P. C., Nielsen, M. C., Gloriam, D. E., Frimurer, T. M., Ulven, T., and Rosenkilde, M. M. (2012) Modulation in selectivity and allosteric properties of small-molecule ligands for CC-chemokine receptors. *J. Med. Chem.* **55,** 8164–8177
32. Heydorn, A., Ward, R. J., Jorgensen, R., Rosenkilde, M. M., Frimurer, T. M., Milligan, G., and Kostenis, E. (2004) Identification of a novel site within G protein α subunits important for specificity of receptor-G protein interaction. *Mol. Pharmacol.* **66,** 250–259
33. Chalikiopoulos, A., Thiele, S., Malmgaard-Clausen, M., Rydberg, P., Isberg, V., Ulven, T., Frimurer, T. M., Rosenkilde, M. M., and Gloriam, D. E. (2013) Structure-activity relationships and identification of optmized CC-chemokine receptor CCR1, 5, and 8 metal-ion chelators. *J. Chem. Inf. Model.* **53,** 2863–2873
34. Jensen, P. C., Thiele, S., Ulven, T., Schwartz, T. W., and Rosenkilde, M. M. (2008) Positive versus negative modulation of different endogenous chemokines for CC-chemokine receptor 1 by small molecule agonists through allosteric versus orthosteric binding. *J. Biol. Chem.* **283,** 23121–23128
35. Thiele, S., Steen, A., Jensen, P. C., Mokrosinski, J., Frimurer, T. M., and Rosenkilde, M. M. (2011) Allosteric and orthosteric sites in CC chemokine receptor (CCR5), a chimeric receptor approach. *J. Biol. Chem.* **286,** 37543–37554
36. Ballesteros, J. A., and Weinstein, H. (1995) Integrated methods for the construction of three-dimensional models and computational probing of structure-function relations in G protein-coupled receptors. In *Methods in Neurosciences* (Stuart, C. S., ed) pp. 366–428, Academic Press, New York
37. Baldwin, J. M. (1993) The probable arrangement of the helices in G protein-coupled receptors. *EMBO J.* **12,** 1693–1703
38. Schwartz, T. W. (1994) Locating ligand-binding sites in 7TM receptors by protein engineering. *Curr. Opin. Biotechnol.* **5,** 434–444
39. Gadhe, C. G., Balupuri, A., and Cho, S. J. (2015) *In silico* characterization of binding mode of CCR8 inhibitor: homology modeling, docking and membrane based MD simulation study. *J. Biomol. Struct. Dyn.* **33,** 2491–2510
40. Blanpain, C., Lee, B., Vakili, J., Doranz, B. J., Govaerts, C., Migeotte, I., Sharron, M., Dupriez, V., Vassart, G., Doms, R. W., and Parmentier, M. (1999) Extracellular cysteines of CCR5 are required for chemokine binding, but dispensable for HIV-1 coreceptor activity. *J. Biol. Chem.* **274,** 18902–18908
41. Limatola, C., Di Bartolomeo, S., Catalano, M., Trettel, F., Fucile, S., Castellani, L., and Eusebi, F. (2005) Cysteine residues are critical for chemokine receptor CXCR2 functional properties. *Exp. Cell Res.* **307,** 65–75
42. Leong, S. R., Kabakoff, R. C., and Hébert, C. A. (1994) Complete mutagenesis of the extracellular domain of interleukin-8 (IL-8) type A receptor identifies charged residues mediating IL-8 binding and signal transduction. *J. Biol. Chem.* **269,** 19343–19348
43. Ai, L. S., and Liao, F. (2002) Mutating the four extracellular cysteines in the chemokine receptor CCR6 reveals their differing roles in receptor trafficking, ligand binding, and signaling. *Biochemistry* **41,** 8332–8341
44. Rummel, P. C., Thiele, S., Hansen, L. S., Petersen, T. P., Sparre-Ulrich, A. H., Ulven, T., and Rosenkilde, M. M. (2013) Extracellular disulfide bridges serve different purposes in two homologous chemokine receptors, CCR1 and CCR5. *Mol. Pharmacol.* **84,** 335–345
45. Rosenbaum, D. M., Cherezov, V., Hanson, M. A., Rasmussen, S. G., Thian, F. S., Kobilka, T. S., Choi, H. J., Yao, X. J., Weis, W. I., Stevens, R. C., and Kobilka, B. K. (2007) GPCR engineering yields high-resolution structural insights into β2-adrenergic receptor function. *Science* **318,** 1266–1273
46. Schneider, T. D., and Stephens, R. M. (1990) Sequence logos: a new way to display consensus sequences. *Nucleic Acids Res.* **18,** 6097–6100
47. Burg, J. S., Ingram, J. R., Venkatakrishnan, A. J., Jude, K. M., Dukkipati, A., Feinberg, E. N., Angelini, A., Waghray, D., Dror, R. O., Ploegh, H. L., and Garcia, K. C. (2015) Structural biology. Structural basis for chemokine recognition and activation of a viral G protein-coupled receptor. *Science* **347,** 1113–1117
48. Kledal, T. N., Rosenkilde, M. M., and Schwartz, T. W. (1998) Selective recognition of the membrane-bound CX3C chemokine, fractalkine, by the human cytomegalovirus-encoded broad-spectrum receptor US28. *FEBS Lett.* **441,** 209–214
49. Neote, K., DiGregorio, D., Mak, J. Y., Horuk, R., and Schall, T. J. (1993) Molecular cloning, functional expression, and signaling characteristics of a C-C chemokine receptor. *Cell* **72,** 415–425
50. Gao, J. L., and Murphy, P. M. (1994) Human cytomegalovirus open reading frame US28 encodes a functional β chemokine receptor. *J. Biol. Chem.* **269,** 28539–28542
51. Peeters, M. C., van Westen, G. J., Li, Q., and IJzerman, A. P. (2011) Importance of the extracellular loops in G protein-coupled receptors for ligand recognition and receptor activation. *Trends Pharmacol. Sci.* **32,** 35–42
52. Avlani, V. A., Gregory, K. J., Morton, C. J., Parker, M. W., Sexton, P. M., and Christopoulos, A. (2007) Critical role for the second extracellular loop in the binding of both orthosteric and allosteric G protein-coupled receptor ligands. *J. Biol. Chem.* **282,** 25677–25686
53. May, L. T., Leach, K., Sexton, P. M., and Christopoulos, A. (2007) Allosteric modulation of G protein-coupled receptors. *Annu. Rev. Pharmacol. Toxicol.* **47,** 1–51
54. Govaerts, C., Bondue, A., Springael, J. Y., Olivella, M., Deupi, X., Le Poul, E., Wodak, S. J., Parmentier, M., Pardo, L., and Blanpain, C. (2003) Activation of CCR5 by chemokines involves an aromatic cluster between transmembrane helices 2 and 3. *J. Biol. Chem.* **278,** 1892–1903
55. Rosenkilde, M. M., Andersen, M. B., Nygaard, R., Frimurer, T. M., and Schwartz, T. W. (2007) Activation of the CXCR3 chemokine receptor through anchoring of a small molecule chelator ligand between TM-III, -IV, and -VI. *Mol. Pharmacol.* **71,** 930–941
56. Casarosa, P., Bakker, R. A., Verzijl, D., Navis, M., Timmerman, H., Leurs, R., and Smit, M. J. (2001) Constitutive signaling of the human cytomegalovirus-encoded chemokine receptor US28. *J. Biol. Chem.* **276,** 1133–1137
57. McLean, K. A., Holst, P. J., Martini, L., Schwartz, T. W., and Rosenkilde, M. M. (2004) Similar activation of signal transduction pathways by the herpesvirus-encoded chemokine receptors US28 and ORF74. *Virology* **325,** 241–251
58. Needleman, S. B., and Wunsch, C. D. (1970) A general method applicable to the search for similarities in the amino acid sequence of two proteins. *J. Mol. Biol.* **48,** 443–453
59. Abagyan, R., Totrov, M., and Kuznetsov, D. (1994) ICM—a new method for protein modeling and design: applications to docking and structure prediction from the distorted native conformation. *J. Comput. Chem.* **15,** 488–506
60. Graham, F. L., and van der Eb, A. J. (1973) A new technique for the assay of infectivity of human adenovirus 5 DNA. *Virology* **52,** 456–467
61. Kostenis, E., Zeng, F. Y., and Wess, J. (1998) Functional characterization of a series of mutant G protein αq subunits displaying promiscuous receptor coupling properties. *J. Biol. Chem.* **273,** 17886–17892
62. Cheng, Y., and Prusoff, W. H. (1973) Relationship between the inhibition constant (K1) and the concentration of inhibitor which causes 50 per cent inhibition (I50) of an enzymatic reaction. *Biochem. Pharmacol.* **22,** 3099–3108
63. Abagyan, R., Batalov, S., Cardozo, T., Totrov, M., Webber, J., and Zhou, Y. (1997) Homology modeling with internal coordinate mechanics: deformation zone mapping and improvements of models via conformational search. *Proteins* **1,** 29–37
64. Crooks, G. E., Hon, G., Chandonia, J. M., and Brenner, S. E. (2004) WebLogo: a sequence logo generator. *Genome Res.* **14,** 1188–1190